Nonlinear Dyn (2015) 82:1393–1398
DOI 10.1007/s11071-015-2246-3

ORIGINAL PAPER

Controllable behaviors of Peregrine soliton with two peaks in a birefringent fiber with higher-order effects

Ji-tao Li · Jin-zhong Han · Yuan-dong Du · Chao-Qing Dai

Received: 15 April 2015 / Accepted: 23 June 2015 / Published online: 7 July 2015

Abstract A coupled variable-coefficient higher-order nonlinear Schrödinger equation in birefringent fiber is discussed, and an analytical Peregrine soliton solution with two peaks is derived by means of the Darboux transformation method. The controllable behaviors of this Peregrine soliton with two peaks are investigated in a periodic dispersion system and a dispersion decreasing fiber with exponential profile. In these systems, the effective propagation distance Z appears a maximum Z_{m}. Comparing this maximum with values of peak location Z_{p}, the initial excitation, peak excitation, rear excitation and periodic excitation are constructed.

Keywords Coupled higher-order nonlinear Schrödinger equation · Birefringent fiber · Peregrine soliton with two peaks

1 Introduction

Nonlinear wave excitations and various solitons, such as autonomous soliton [1,2], shock waves [3], spatial soliton [4], dipole soliton [5], Kuznetsov-Ma soliton [6] and light bullet [7], exist in various nonlinear optical systems. As one of research focus, dynamical behaviors of rogue waves (RWs) [8] were intensively studied in different domains of physics, especially in fluid dynamics [9], nonlinear optical systems [10] and plasmas [11].

As is well known, the Peregrine solitons (PS) [12] have been reported as one of the theoretical prototypes to describe RWs. In optics, Solli et al. [13] firstly introduced the concept of RW in a photonic crystal fiber. After then, many groups experimentally observed optical rogue soliton in different contexts [14–16]. Because it is significant and interesting to understand theoretically the control and use of RWs, many authors [17–19] investigated controllable behaviors of RWs. However, these investigation are all related to the standard nonlinear Schrödinger equation (NLSE), and the higher-order effects such as the self-steepening (SS) and self-frequency shift (SFS) are less considered when authors studied RWs.

In this paper, we considered a coupled NLSE with higher-order effects and discussed controllable behaviors of PS with two peaks in a birefringent fiber. Comparing the maximal effective propagation distance Z_{m} with values of peak location Z_{p}, controllable behaviors, such as the initial excitation, peak excitation, rear excitation and periodic excitation, are discussed in a periodic dispersion system and a dispersion decreasing fiber (DDF) with exponential profile.

J. Li · J. Han (✉)· Y. Du
School of Physics and Electromechanical Engineering, Zhoukou Normal University, Zhoukou 466001, People's Republic of China
e-mail: hanjinzhong@zknu.edu.cn

C.-Q. Dai
School of Sciences, Zhejiang Agriculture and Forestry University, Lin'an 311300, Zhejiang, People's Republic of China

2 Model and Peregrine soliton solution

Considering the presence of birefringence, single-mode fibers are actually bimodal. This birefringence creates two principal transmission axes within the fiber known as the fast and slow axes. When traveling in a medium, an ultrashort light pulse will induce a varying refractive index of the medium, which will produce a phase shift in the pulse called self-phase modulation (SPM). When two or more optical fields with different frequencies co-propagate in a fiber, the cross-phase modulation (XPM) will be produced through the optical Kerr effect. When short pulse is considered (nearly 50fs), the third-order dispersion (TOD), which will produce asymmetrical broadening in the time domain for the ultrashort soliton pulses [20], cannot be neglected. Moreover, the higher-order nonlinear effects such as the SS [21] and SFS [22] must be considered.

In a real fiber, the variation of the fiber geometry (diameter fluctuations, etc.) brings to the inhomogeneous core medium [23] and thus the governing equation is the following higher-order coupled NLSE with variable coefficients [24]

$$\begin{aligned} &\mathrm{i}q_{jz} - \frac{1}{2}\beta_2(z)q_{jtt} - \gamma(z)\left(\sum_{n=1}^{2} a_{nj}|q_n|^2\right)q_j \\ &+ \mathrm{i}\beta_3(z)q_{jttt} + \mathrm{i}\chi(z)\left(\sum_{n=1}^{2} a_{nj}|q_n|^2\right)q_{jt} \\ &+ \mathrm{i}\delta(z)\left(\sum_{n=1}^{2} a_{nj}q_{nt}q_j^*\right)q_j + \mathrm{i}\Gamma(z)q_j = 0, \end{aligned} \tag{1}$$

where $q_j(z,t)$ with $j = 1,2$ denote two normalized complex mode fields, z and t represent dimensionless propagation and retarded time. In Eq. (1), $\beta_2(z)$, $\gamma(z)$, $\beta_3(z)$, $\chi(z)$, $\delta(z)$ and $\Gamma(z)$ are coefficients of group velocity dispersion (GVD), the nonlinearly coupled terms of the SPM and XPM, TOD, SS and SFS, and loss and gain, respectively. The $(*)$ denotes the complex conjugate, and subscripts z and t denote the derivatives with respect to z and t. The constants a_{nj} decide the ratio of the coupling strengths of the XPM to the SPM. For linearly polarized eigenmodes $a_{11} = a_{22} = 1, a_{12} = a_{21} = 2/3$, whereas for circularly polarized modes $a_{11} = a_{22} = 1, a_{12} = a_{21} = 2$ with elliptically polarized eigenmodes $a_{11} = a_{22} = 1, 2/3 < a_{12} = a_{21} < 2$ [25]. In Ref. [24], dispersion management and cascade compression of femtosecond nonautonomous soliton have been discussed via Darboux transformation method; however, the PS has not been discussed. Note that here we consider the special case with the same wavelength for both polarization components. Moreover, we neglect the degenerate four-wave mixing. If the fiber length $L \gg L_B$ (beat length), the four-wave-mixing term changes sign often and its contribution averages out to zero. In highly birefringent fibers ($L_B \sim 1$ cm typically), the four-wave-mixing term can often be neglected for this reason [26].

When all coefficients in Eq. (1) are constant, bright soliton has been obtained [27]. Moreover, the coupled NLSE with higher-order effects can also describe short pulse propagation in the dual-core photonic crystal fiber [28,29]. Different from the numerical study in Refs. [28,29], here we analytically study the propagation of soliton. The variable-coefficient model here can describe more general situation than the constant-coefficient one in Ref. [27]; however, the solving procedure for the variable-coefficient model (1) here is more complicated than that for the constant-coefficient one in Ref. [27]. Considering bright soliton has been discussed in Ref. [27], we focus on another new soliton structure, that is, the novel PS with two peaks.

Under the condition

$$\begin{aligned} &\beta_3(z) : \beta_2(z) : \gamma(z) : \chi(z) : \delta(z) = 1 : 2\left(\frac{k}{s\gamma_3} - 3p\right) : \\ &-\frac{k^2[ps(2a_f + s_a) + k)}{s\gamma_3 A_0^2}\exp\left[2\int_0^z \Gamma(s)\mathrm{d}s\right] : \\ &-\frac{2k^2 a_f}{A_0^2\gamma_3}\exp\left[2\int_0^z \Gamma(s)\mathrm{d}s\right] : \\ &-\frac{k^2 s_a}{A_0^2\gamma_3}\exp\left[2\int_0^z \Gamma(s)\mathrm{d}s\right], \end{aligned} \tag{2}$$

if we use the transformation

$$\begin{aligned} \begin{Bmatrix} q_1 \\ q_2 \end{Bmatrix} &= A(z)\exp\left[\mathrm{i}\phi(z,t)\right]Q\left[Z(z), T(t)\right] \\ &\times \begin{Bmatrix} |a_{22} - a_{12}|^{\frac{1}{2}} \\ |a_{11} - a_{21}|^{\frac{1}{2}} e^{\mathrm{i}\vartheta} \end{Bmatrix}, \end{aligned} \tag{3}$$

with the amplitude $A(z) = A_0\exp\left[-\int_0^z \Gamma(s)\mathrm{d}s\right]$, phase $\phi(z,t) = p\left[t + p\left(\frac{k}{s\gamma_3} - 4p\right)\int_0^z \beta_3(s)\mathrm{d}s\right]$, the effective propagation distance $Z(z) = -\frac{k^3}{s\gamma_3}\int_0^z \beta_3(s)\mathrm{d}s$, intermediate variable $T(t) = k[t + p\left(9p - \frac{2k}{s\gamma_3}\right)\int_0^z \beta_3(s)\mathrm{d}s]$ and constants k, p, ϑ, then Eq. (1) can be transformed into the constant-coefficient higher-order NLSE [30]

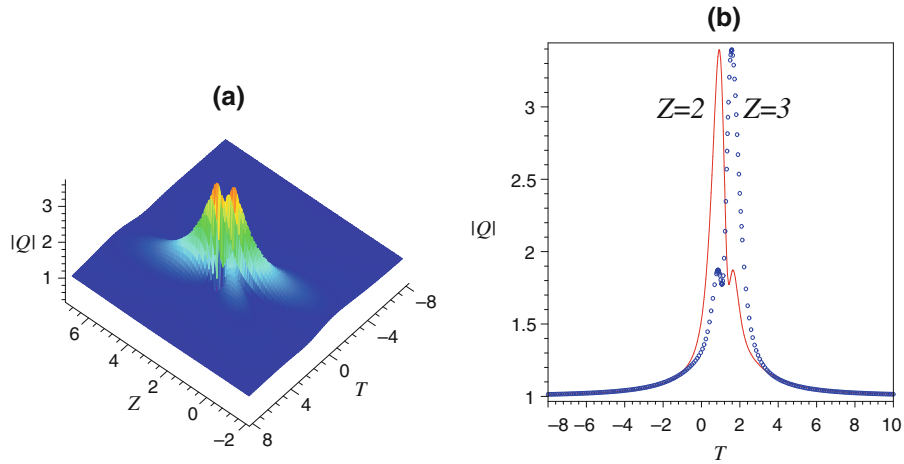

Fig. 1 (Color online) **a** The PS with two peaks for Eq.(4) in the $Z-T$ coordinates and **b** the corresponding sectional plot at $Z=2$ and $Z=3$. Parameters are chosen as $\gamma_3=0.2, a_f=1, s_a=1, s=0.25, T_0=5, Z_0=10$

$$\mathrm{i}Q_Z+\frac{1}{2}Q_{TT}+|Q|^2Q+\mathrm{i}s[a_f Q(|Q|^2)_T +s_a(|Q|^2Q)_T-\gamma_3 Q_{TTT}]=0, \tag{4}$$

with three independent parameters s_a, a_f and γ_3 controlling the relative contribution of SFS, SS and TOD.

Note that the one-to-one correspondence (3) has been constructed between the complicated variable-coefficient model (1) and the terse constant-coefficient model (4). Therefore, various solutions of Eq.(1) can be obtained by means of the relation (3) and solutions of Eq.(4). Obviously, the advantage of this method is that the correspondence (3) simplifies the solving procedure of complicated variable-coefficient model (1) by firstly solving easier constant-coefficient model (4).

According to the modified Darboux transformation technique in Ref. [30], we can obtain the novel PS solution with two peaks as follows

$$\begin{Bmatrix} q_1 \\ q_2 \end{Bmatrix} = A(z)\exp\{\mathrm{i}[\phi(z,t)+Z]\} \times\left\{\frac{4}{D}(1+2\mathrm{i}Z')-1+\frac{\mathrm{i}s}{D^2}\left[M(Z',T')-\mathrm{i}N(Z',T')\right]\right\} \times\begin{Bmatrix} |a_{22}-a_{12}|^{\frac{1}{2}} \\ |a_{11}-a_{21}|^{\frac{1}{2}}e^{\mathrm{i}\vartheta} \end{Bmatrix}, \tag{5}$$

where $D=1+4Z'^2+4T'^2$, $M(Z',T')=8T'\{4(a_f+6\gamma_3+2s_a)T'^2+12[a_f+2(\gamma_3+s_a)]Z'^2-3a_f-6\gamma_3-4s_a\}$, $N(Z',T')=32(3a_f+6\gamma_3+5s_a)T'Z'$ with $Z'=Z-sZ_0$, $T'=T-sT_0$. Here these expressions of Z, T and ϕ are shown below Eq. (3), and Z_0 and T_0 determine the center of solution in $Z-T$ coordinates.

3 Controllable behaviors of PS with two peaks

The higher-order NLSE (4) has PS solution as [30]

$$Q=\left\{\frac{4}{D}(1+2\mathrm{i}Z')-1+\frac{\mathrm{i}s}{D^2}[M(Z',T') -\mathrm{i}N(Z',T')]\right\}\exp(\mathrm{i}Z). \tag{6}$$

As shown in Fig. 1, this solution becomes asymmetric relative to mirror images along axes $Z=0$ and $T=0$ and possesses two-peak structure. It is also one kind of wave that appeared from nowhere and disappeared without a trace (WANDT) like the original PS [31].

From solution (5), we know its core is solution (6). However, solution (5) not only possesses the property of WANDT, but also can be controlled to realize different excitations, which does not appear for solution (6) in the frame of higher-order NLSE (4). This new property originates from the restraint for value of Z by the expression $Z(z)=-\frac{k^3}{s\gamma_3}\int_0^z\beta_3(s)\mathrm{d}s$, that is, Z is not an arbitrary value from 0 to infinity. Here, we choose $a_{11}=a_{22}=1, a_{12}=a_{21}=2/3$.

We analyze the controllable behaviors of PS solution (6) in the following periodic distributed amplification system with the periodic varying TOD parameter [32]

$$\beta_3(z)=\beta_{30}\cos(\eta z)\exp(-\sigma z), \tag{7}$$

where the parameters η and σ control the rate of TOD change inside the fiber. In particular, the constant TOD can be obtained by $\eta=\sigma=0$. When $\sigma=0$, this

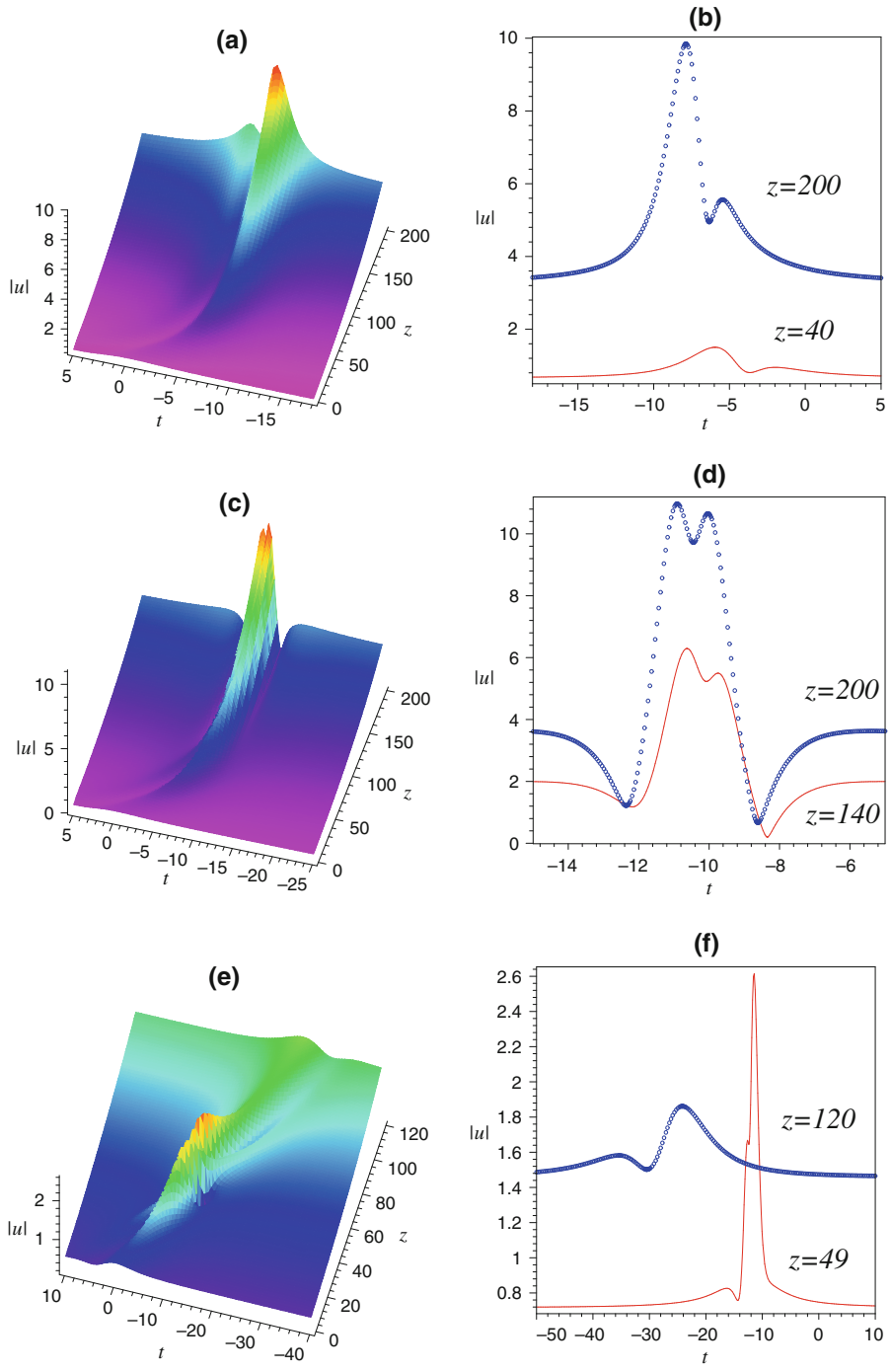

Fig. 2 (Color online) Controllable behaviors of PS with $|u| = |q_1|$ in DDF: **a** initial excitation, **c** peak excitation and **e** rear excitation. **b**, **d** and **f** are sectional plots corresponding to **a**, **c** and **e** at different z. Parameters are chosen as $k = 0.4$, $\beta_{30} = -0.05$, $\Gamma = -0.01$, $A_0 = 0.5$, $p = 1$, $\eta = 0$ with **a** $\sigma = 0.035$, **b** $\sigma = 0.0256$ and **c** $\sigma = 0.005$. Other parameters are chosen as those in Fig. 1

system (7) is the periodic dispersion system [10]. When $\eta = 0$, this system (7) with $\sigma > 0$ is the DDF with exponential profile [33].

In DDF, from expression of Z below Eq.(3), we obtain $Z = -k^3\beta_{30}[1 - \exp(-\sigma z)]/(s\gamma_3\sigma)$. When $\sigma > 0$, the maximum value is $Z_{\mathrm{m}} = -k^3\beta_{30}/(s\gamma_3\sigma)$ as $z \to \infty$. Moreover, peaks of PS appear some fixed locations Z_{p} along the Z-axis in the frame of higher-order NLSE in Fig. 1. Therefore, we can adjust the value of the maximum Z_{m} compared with values of peak loca-

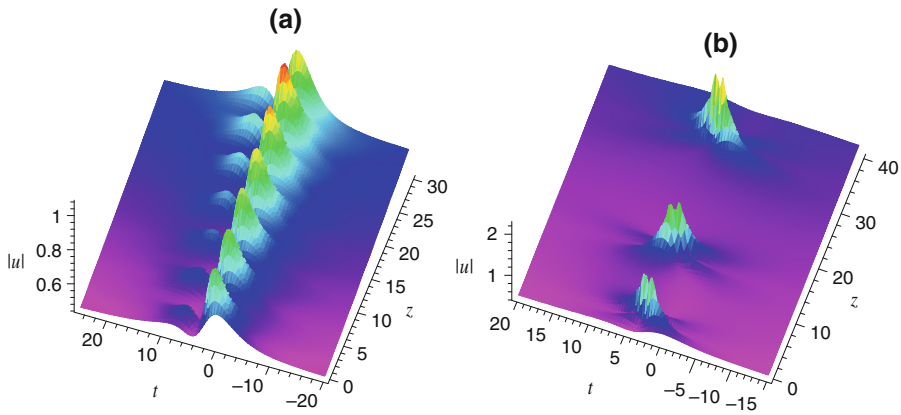

Fig. 3 Controllable behaviors of PS with $|u| = |q_1|$ in periodic system: **a** periodic initial excitation and **b** periodic complete excitation. Parameters are chosen as $\sigma = 0$ with **a** $\eta = 1.2$ and **b** $\eta = 0.2$. Other parameters are chosen as those in Fig. 2

tions Z_p in order to control the degree of excitation of the PS structure in Fig. 1.

When $Z_m < Z_p$, the critical value of exciting PS is not enough. As shown in Figs. 2a, b, the PS is initially excited and maintains this shape self-similarly. If $Z_m = Z_p$, the PS is excited to the magnitude of peak, and sustains its two-peak structure along the propagation distance in a self-similar form (See Fig. 2c, d). When $Z_m > Z_p$, the excitation of rear of PS with two peaks does not finish. The PS is excited to the rear part, and the rear part looks like a tail and sustains its magnitude a long distance from Fig. 2e, f. Thus, the full excitation of the PS cannot be realized.

In periodic dispersion system, from expression of Z below Eq. (3), we obtain $Z = -k^3\beta_{30}\sin(\eta z)/(s\gamma_3\eta)$. This expression hints that Z is limited to the range of $|Z| < |Z_m| = |k^3\beta_{30}/(s\gamma_3\eta)|$. When $|Z_m| < Z_p$, the critical value of exciting PS is not reached, and only initial shape of PS is excited. This maximum is modulated by sin-function, and thus, this initial part appear periodically in Fig. 3a. If $|Z_m| > Z_p$, the PS will be firstly excited at $z = -\arcsin[Z_p s\gamma_3\eta/(\beta_{30}k^3)]/\eta$ and then recur self-similarly in Fig. 3b. From it, we find that the orientation of PS changes alternately, and PS exhibits asymmetric layout relative to mirror image.

From these examples, we know that controllable behaviors can be realized by adjusting the parameter σ in DDF and the parameter η in periodic dispersion system when other parameters are fixed.

4 Conclusions

In summary, we discussed a coupled variable-coefficient higher-order NLSE in birefringent fiber, and obtained an analytical Peregrine soliton solution with two peaks via the Darboux transformation method. Moreover, we studied controllable behaviors of PS with two peaks in a DDF and a periodic dispersion system. In the DDF, the effective propagation distance Z appears a maximum Z_m. Comparing this maximum with values of peak location Z_p, the initial excitation, peak excitation and rear excitation are constructed by adjusting the parameter σ in DDF, and periodic initial excitation and complete excitation are built by modulating the parameter η in periodic dispersion system when other parameters are fixed. These results will stimulate study RWs for shorter pulse width when higher-order effects are considered.

Acknowledgments This work was supported by the Science and Technology Department of Henan province under Grant No. 142300410043, the Education Department of Henan province under Grant No. 13A140113 and the National Natural Science Foundation of China under Grant No. 11404289.

References

1. Mirzazadeh, M., Arnous, A.H., Mahmood, M.F., Zerrad, E., Biswas, A.: Soliton solutions to resonant nonlinear Schrödinger's equation with time-dependent coefficients by trial solution approach. Nonlinear Dyn. **81**, 277–282 (2015)
2. Lü, X., Lin, F., Qi, F.: Analytical study on a two-dimensional Korteweg–de Vries model with bilinear representation, Bäcklund transformation and soliton. Appl. Math. Model. **39**, 3221–3226 (2015)
3. Mirzazadeh, M., Eslami, M., Biswas, A.: 1-Soliton solution of KdV6 equation. Nonlinear Dyn. **80**, 387–396 (2015)
4. Wang, Y.Y., Dai, C.Q., Wang, X.G.: Stable localized spatial solitons in PT-symmetric potentials with power-law nonlinearity. Nonlinear Dyn. **77**, 1323–1330 (2014)
5. Azzouzia, F., Triki, H., Grelu, Ph: Dipole soliton solution for the homogeneous high-order nonlinear Schrödinger equa-

tion with cubic-quintic-septic non-Kerr terms. Appl. Math. Model. **39**, 1300–1307 (2015)
6. Zhu, H.P.: Spatiotemporal solitons on cnoidal wave backgrounds in three media with different distributed transverse diffraction and dispersion. Nonlinear Dyn. **76**, 1651–1659 (2014)
7. Chen, Y.X.: Sech-type and Gaussian-type light bullet solutions to the generalized (3 + 1)-dimensional cubic-quintic Schrodinger equation in PT-symmetric potentials. Nonlinear Dyn. **79**, 427–436 (2015)
8. Broad, W.J.: Rogue Giants at Sea. The New York Times, New York (2006)
9. Chen, W.L., Dai, C.Q., Zhao, L.H.: Nonautonomous superposed Akhmediev breather in water waves. Comput. Fluids **92**, 1 (2014)
10. Dai, C.Q., Zhu, H.P.: Superposed Akhmediev breather of the (3 + 1)-dimensional generalized nonlinear Schrödinger equation with external potentials. Ann. Phys. **341**, 142 (2014)
11. Wang, Y.Y., Li, J.T., Dai, C.Q., Chen, X.F., Zhang, J.F.: Solitary waves and rogue waves in a plasma with nonthermal electrons featuring Tsallis distribution. Phys. Lett. A **377**, 2097 (2013)
12. Peregrine, D.H.: Water waves, nonlinear Schrödinger equations and their solutions. J. Aust. Math. Soc. Ser. B **25**, 16 (1983)
13. Solli, D.R., Ropers, C., Koonath, P., Jalali, B.: Optical rogue waves. Nature **450**, 1054 (2007)
14. Kasparian, J., Béjot, P., Wolf, J.P., Dudley, J.M.: Optical rogue wave statistics in laser filamentation. Opt. Express **17**, 12070 (2009)
15. Kibler, B., Fatome, J., Finot, C., Millot, G., Dias, F., Genty, G., Akhmediev, N., Dudley, J.M.: The Peregrine soliton in nonlinear fibre optics. Nat. Phys. **6**, 790 (2010)
16. Erkintalo, M., Genty, G., Dudley, J.M.: Rogue-wave-like characteristics in femtosecond supercontinuum generation. Opt. Lett. **34**, 2468–2471 (2009)
17. Zhu, H.P.: Nonlinear tunneling for controllable rogue waves in two dimensional graded-index waveguides. Nonlinear Dyn. **72**, 873 (2013)
18. Dai, C.Q., Wang, Y.Y., Zhang, X.F.: Controllable Akhmediev breather and Kuznetsov-Ma soliton trains in PT-symmetric coupled waveguides. Opt. Express **22**, 29862 (2014)
19. Zhong, W.P., Belic, M., Zhang, Y.Q.: Second-order rogue wave breathers in the nonlinear Schrodinger equation with quadratic potential modulated by a spatially-varying diffraction coefficient. Opt. Express **23**, 3708–3716 (2015)
20. Bourkoff, E., Zhao, W., Joseph, R.I., Christodoulides, D.N.: Evolution of femtosecond pulses in single-mode fibers having higher-order nonlinearity and dispersion. Opt. Lett. **12**, 272–274 (1987)
21. Trippenbach, M., Band, Y.B.: Effects of self-steepening and self-frequency shifting on short-pulse splitting in dispersive nonlinear media. Phys. Rev. A **57**, 4791 (1998)
22. Mitschke, F.M., Mollenauer, L.F.: Discovery of the soliton self-frequency shift. Opt. Lett. **11**, 657–659 (1986)
23. Abdullaeev, F.: Theory of Solitons in Inhomogeneous Media. Wiley, New York (1994)
24. Rajan Mani, M.S., Hakkim, J., Mahalingam, A., Uthayakumar, A.: Dispersion management and cascade compression of femtosecond nonautonomous soliton in birefringent fiber. Eur. Phys. J. D **67**, 150 (2013)
25. Chang, C.C., Sardesai, H.P., Weiner, A.M.: Dispersion-free fiber transmission for femtosecond pulses by use of a dispersion-compensating fiber and a programmable pulse shaper. Opt. Lett. **23**, 283–285 (1998)
26. Agrawal, G.P.: Nonlinear Fiber Optics, 5th edn. Academic Press, California (2013)
27. Bhrawy, A.H., Alshaery, A.A., Hilal, E.M., Savescu, M., Milovic, D., Khan, K.R.: Optical solitons in birefringent fibers with spatio-temporal dispersion. Optik **125**, 4935–4944 (2014)
28. Khan, K.R., Bydnik, S., Hall, T.: Tunable all optical switch implemented in a liquid crystal filled dual-core photonic crystal fiber. Prog. Electromagn. Res. M **22**, 179–189 (2012)
29. Khan, K.R., Wu, T.: Short pulse propagation in wavelength selective index guided photonic crystal fiber coupler. IEEE J. Sel. Top. Quantum Electron. **14**, 752–757 (2008)
30. Ankiewicz, A., Devine, N., Akhmediev, N.: Are rogue waves robust against perturbations? Phys. Lett. A **373**, 3997–4000 (2009)
31. Akhmediev, N., Ankiewicz, A., Taki, M.: Waves that appear from nowhere and disappear without a trace. Phys. Lett. A **373**, 675–678 (2009)
32. Dai, C.Q., Wang, Y.Y., Zhang, J.F.: Analytical spatiotemporal localizations for the generalized (3 + 1)-dimensional nonlinear Schrödinger equation. Opt. Lett. **35**, 1437–1439 (2010)
33. Dai, C.Q., Wang, Y.Y., Wang, X.G.: Ultrashort self-similar solutions of the cubic-quintic nonlinear Schrödinger equation with distributed coefficients in the inhomogeneous fiber. J. Phys. A Math. Theor. **44**, 155203 (2011)